Publisher's version: Daneshvar, S., Sun, M. & Tousignant, K. (2020). Stress concentration factors for RHS-to-RHS X-connections near an open chord end. Journal of Constructional Steel Research 175: 106352.
https://doi.org/10.1016/j.jcsr.2020.106352

Stress Concentration Factors for RHS-to-RHS X-Connections near an Open Chord End

by

Sara Daneshvar, Min Sun*
Department of Civil Engineering, University of Victoria, Victoria, British Columbia V8P 5C2, Canada
and
Kyle Tousignant
Department of Civil & Resource Engineering, Dalhousie University, Halifax, NS, B3H 4R2, Canada

Abstract

This paper presents an experimental and finite-element (FE) study to determine stress concentration factors (SCFs) for directly welded rectangular hollow section (RHS)-to-RHS axially loaded X-connections near an open chord end. Two-hundred and fifty-six FE models of RHS-to-RHS X-connections, with varied chord end distance-to-width (e/b_0), branch-to-chord width (β), branch-to-chord thickness (τ), and chord slenderness (2γ) ratios were modelled and analyzed by using commercial software. The analysis was performed under quasi-static axial compression force(s) applied to the branch(es) and validated by comparison of strain concentration factors (SCNFs) to SCNFs obtained from two large-scale experimental tests. For all 256 connections, SCFs were determined at five critical hot spots on the side of the connection near the open chord end. The SCFs were found to vary as a function of e/b_0, 2γ and β. Existing formulae in CIDECT DG8 to predict SCFs in directly welded RHS-to-RHS axially loaded X-connections are shown to be conservative when applied to a connection near an open chord end. SCF reduction factors (ψ), and a parametric formula to estimate ψ based on e/b_0, 2γ and β, are derived.

Keywords

Rectangular hollow sections; X-connections; end effects; stress concentration factors; fatigue design; cap plates.

*Corresponding Author. E-mail: msun@uvic.ca

1. Introduction

Over the last 60 years, substantial work has been carried out to develop design recommendations for rectangular hollow section (RHS)-to-RHS and circular hollow section (CHS)-to-CHS connections under static [1-4] and fatigue [5,6] loading. These recommendations are the basis for design rules for tubular structures in Canada (via [7,8]), the United States (via [9-11]), and Europe (via [12]).

The design rules in [9-12] are predicated upon a hollow structural section (HSS) (RHS or CHS) chord member that is sufficiently long on both sides of the connection [i.e. the "end distance" (*e*), in Fig. 1a, is large] to avoid the effect of the chord boundary conditions (i.e. "end effects") on the connection behaviour [13].

Thus, at present, there are few established design rules for cases in which an HSS branch(es) is situated near an HSS chord end (i.e. an "end connection"), as shown in Figs. 1b,c. When these arise (as they often do), designers invariably resort to strengthening the connection via cap plates (or end plates), doubler plates, or diaphragms [14]. This can be an expensive and inefficient practice, for both static loading and fatigue. For fabrication, un-strengthened (i.e. directly welded) connections are almost always preferred.

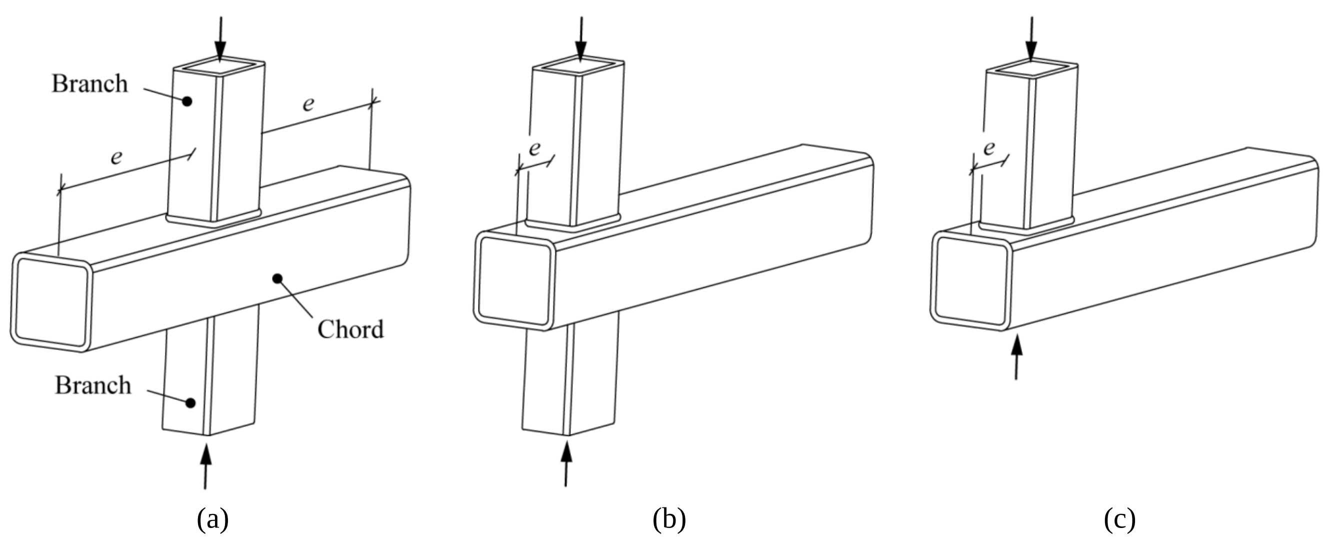

Fig. 1. RHS-RHS X-connections: (a) standard connection; (b) and (c) end connections

As a step towards addressing this problem, this paper presents a study to determine stress concentration factors (SCFs) for directly welded RHS-to-RHS axially loaded X-connections near an *open* chord end (e.g. Figs.

1b,c). Two large-scale experiments are used to validate finite element (FE) models, and a parametric FE study is performed. The FE study consists of 256 FE models with variations in non-dimensional parameters [i.e. chord slenderness ($2\gamma = b_0/t_0$, where b_0 = chord width and t_0 = chord thickness), branch-to-chord width ratio ($\beta = b_1/b_0$, where b_1 is the branch width), branch-to-chord thickness ratio ($\tau = t_1/t_0$, where t_1 is the branch thickness] and e (on *one side* of the of the connection) = 0.1, 0.25, 1.0 and 3.0 times b_0. This terminology (for RHS-to-RHS connections) is illustrated in Fig. 2]. For each connection, SCFs are determined. Existing formulae to predict SCFs in directly welded RHS-to-RHS X-connections given in CIDECT DG8 [5] are evaluated and shown to be over-conservative; hence, SCF reduction coefficients (ψ) – and parametric formula to estimate ψ (based on e/b_0, 2γ and β) – are derived.

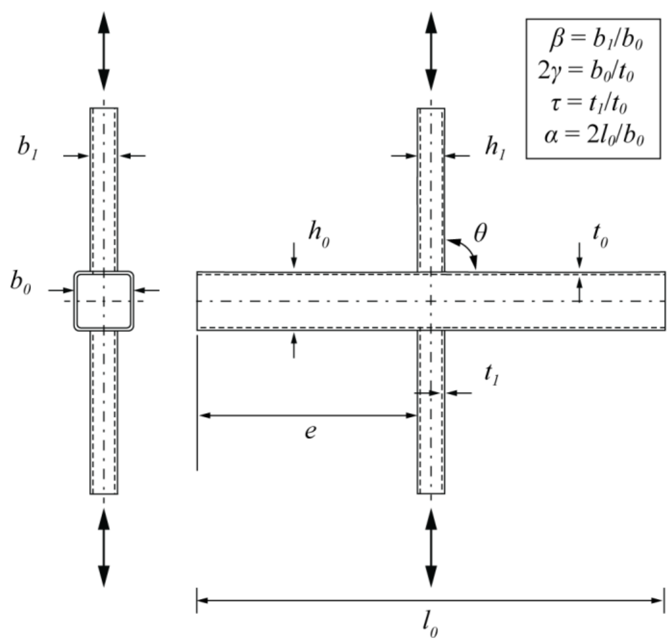

Fig. 2. RHS-to-RHS X-connection terminology

2. Recent Research on HSS End Connections

Contemporary research on directly welded HSS-to-HSS end connections can be attributed to work by van der Vegte and Makino [15]. van der Vegte and Makino [15] studied CHS-to-CHS axially loaded T- and X-connections with variations in chord slenderness ($2\gamma = d_0/t_0$, where d_0 = chord diameter), branch-to-chord diameter ratio ($\beta = d_1/d_0$, where d_1 = branch diameter), chord length parameter ($\alpha = 2l_o/d_o$, where l_o = chord length), and chord boundary conditions [which were modelled as either "free" (simulating an open end) or "fixed" (simulating a capped end)]. This terminology (for CHS-to-CHS connections) is illustrated in Fig. 3.

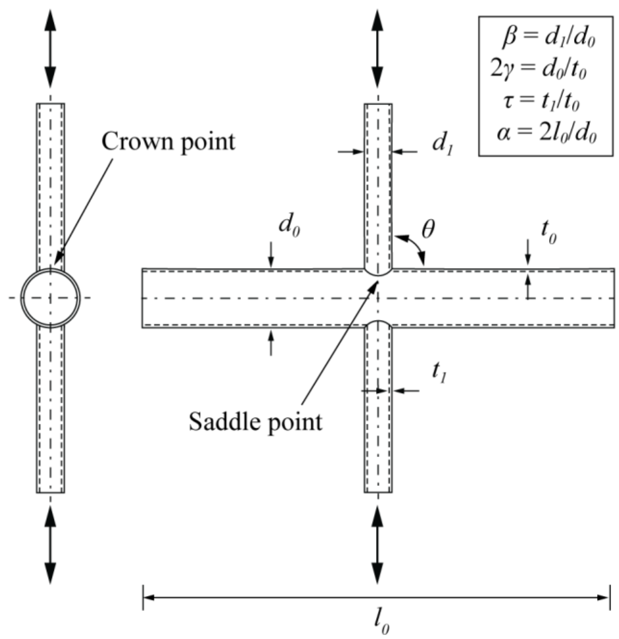

Fig. 3. CHS-to-CHS X-connection terminology

In their research, van der Vegte and Makino [15] showed that the static strength of a CHS-to-CHS axially loaded T- or X-connection with low α, high 2γ, high β, and open chord ends could be much less than that of a similar connection with high α. To prevent end effects, they proposed simple limits of $\alpha \geq 20$ (for chords with $2\gamma > 25$) and $\alpha \geq 12$ (for chords with $2\gamma \leq 25$). These limits imply a minimum end distance (e_{min}), which was later confirmed for transverse branch plate-to-CHS T- and X-connections by Voth and Packer [16,17].

In response to this research [15-17], an amendment was made to EN 1993-1-8 [12] (via prEN1993-1-8 Clause 9.1.2(10) [18]), which stipulates:

> "For joints with a chord end not connected to other members, the chord end shall be at a distance of at least $(2\gamma/10)d_0$ from the heel or toe of the closest brace, with a minimum of $2.5d_0$. For RHS chords, substitute d_0 by the largest of b_0 or h_0. Otherwise, the end shall be welded to a cap plate with a thickness of at least $1.5t_0$, at a minimum distance of $0.5d_0(1 - \beta)$ or $0.5b_0(1 - \beta)$ from the brace toe or heel of the joint".

Note that the term “brace” in prEN1993-1-8 [18] is synonymous with the term “branch” (see Fig. 1a) (used herein).

The formula for e_{min} implied in the amendment (prEN1993-1-8 Clause 9.1.2(10) [18]) is verified for CHS-to-CHS and plate-to-CHS connections [15-17], and for welds in CHS-to-CHS connections designed as “fit-for-purpose” [19]; however, a speculative transcription (i.e. “substitute d_0 by the largest of b_0 or h_0”) [18] was made for application to HSS connections with RHS chords. Additionally, the research discussed so far [15-17,19] caters only to connections that are symmetrical about the branch(es).

These issues were addressed by Fan and Packer [14], who experimentally studied the static strength of RHS-to-RHS axially loaded X-connections near an open chord end (on one side only). Akin to previous work [15,20-23], Fan and Packer [14] found that the static strengths of such connections near an open chord end were often much less than those of “standard” (or “control”) connections with long chords ($e \geq 3b_0$, conservatively, on both sides). A yield-line model was developed, from which e_{min} was derived (for HSS connections with RHS chords). This research supported the e_{min} requirement already present in AISC 360-16 [9] Table K3.2A for RHS-to-RHS truss connections (Eq. 1), which is (a) based on the “chord face plastification” limit state and (b) clearly much different (i.e. less) than e_{min} implied in prEN1993-18 Clause 9.1.2(10).

$$e_{\min} = b_0\sqrt{1-\beta} \quad (1)$$

While both prEN1993-1-8 Clause 9.1.2(10) [18] and AISC 360-16 (via the Commentary to Chapter K) [9] recognize providing a cap plate as a “commonly accepted alternative” to providing $e \geq e_{min}$, AISC 360-16 [9] also permits a reduction in the predicted connection strength by 50% for RHS-to-RHS or plate-to-RHS connections (as another alternative).

Bu and Packer [13] have shown recently that Eq. (1) is, in fact, unconservative, since it is based solely on “chord face plastification” and does not consider other limit states. Based on their research, which considered “chord side wall buckling” in addition to “chord face plastification”, Bu and Packer [13] proposed: (a) a new limit of $e_{min} = 0.75b_0$ for HSS connections with RHS chords and (b) a reduction in strength by 40% (instead of 50%) if $e < e_{min} = 0.75b_0$.

While research has hence aimed to establish design guidance for directly welded HSS "end connections" under static loading [13-17,19-23], research on "end connections" under fatigue loading is rare. Efthymiou and Durkin [24] showed that SCFs in CHS-to-CHS connections with short chords (i.e. low α) were often much smaller than those in "standard" connections (with long chords), which has formed the basis of some of the SCF formulae for CHS-to-CHS axially loaded X-connections in CIDECT DG8 [5] (which are discussed in Section 3.1 of this paper). However, like most previous research [15-17,19], Efthymiou and Durkin's [24] work catered only to connections that are symmetrical about the branch(es).

3. Design of HSS Connections for Fatigue

For HSS-to-HSS connections subjected to fatigue, design is commonly done according to the "hot spot stress method" in CIDECT DG8 [5]. The procedure to apply this method is as follows:

1. Calculate the nominal stress ranges in the branch(es) and chord under service conditions.
2. Calculate the SCFs at the critical (hot spot) locations (for which formulae are provided in [5]).
3. Calculate the hot spot stress range at the critical locations (equal to: nominal stress range × SCF).
4. Determine the fatigue life of the connection by using hot-spot-stress vs. fatigue life (S-N) curves.

The SCFs needed for 2. are functions of connection geometry (e.g. α, β and 2γ) that can be determined by connection testing or FE analysis, or – for standard connections (e.g. Fig 1a) – by using formulae provided in CIDECT DG8 [5] or other HSS design guides. The terms "hot spot stress" and "hot spot stress range" used herein are synonymous with the terms "geometric stress" and "geometric stress range", which may be more familiar to some readers.

3.1. CHS X-Connections

For CHS-to-CHS axially loaded X-connections, the CIDECT DG8 [5] formulae for SCFs consider critical (hot spot) stress locations at the crown and saddle points (see Fig. 3). These formulae are presented in Eqs. (2)-(11) using the nomenclature from CIDECT [5].

- For the chord:

$$SCF_{ch\_saddle,ax} = X_1 \cdot F_2 \tag{2}$$

$$SCF_{ch\_crown,ax} = X_2 \tag{3}$$

where $SCF_{,ch\_saddle,ax}$ = chord SCF at the saddle point; $SCF_{ch\_crown,ax}$ = chord SCF at the crown point; and F_2 = reduction factor to account for “end effects” [24].

- For the branch(es):

$$SCF_{b\_saddle,ax} = X_3 \cdot F_2 \tag{4}$$

$$SCF_{b\_crown,ax} = X_4 \tag{5}$$

where $SCF_{,b\_saddle,ax}$ = branch SCF at the saddle point; and $SCF_{b\_crown,ax}$ = branch SCF at the crown point.

The parameters X_1, X_2, X_3, X_4 and F_2 are given as:

$$X_1 = 3.87 \cdot \gamma \cdot \tau \cdot \beta \left[1.10 - \beta^{1.8}\right] \cdot (\sin\theta)^{1.7} \tag{6}$$

$$X_2 = \gamma^{0.2} \cdot \tau \left[2.65 + 5 \cdot (\beta - 0.65)^2\right] - 3 \cdot \tau \cdot \beta \cdot \sin\theta \tag{7}$$

$$X_3 = 1 + 1.9 \cdot \gamma \cdot \tau^{0.5} \cdot \beta^{0.9} \cdot \left(1.09 - \beta^{1.7}\right) \cdot \sin^{2.5}\theta \tag{8}$$

$$X_4 = 3 + \gamma^{1.2} \cdot \left[0.12 \cdot \exp(-4 \cdot \beta) + 0.011 \cdot \beta^2 - 0.045\right] \tag{9}$$

If $\alpha \geq 12$: $$F_2 = 1.0 \tag{10}$$

If $\alpha < 12$: $$F_2 = 1 - \left(1.43 \cdot \beta - 0.97 \cdot \beta^2 - 0.03\right) \cdot \gamma^{0.04} \cdot \exp\left(-0.71 \cdot \gamma^{-1.38} \cdot \alpha^{2.5}\right) \tag{11}$$

where θ = acute angle between the branch and chord (in degrees) (see Fig. 3).

Eqs. (2)-(11) are valid within the range $0.2 \leq \beta \leq 1.0$, $15 \leq 2\gamma \leq 64$, $0.2 \leq \tau \leq 1.0$, $4 \leq \alpha \leq 40$, and $30° \leq \theta \leq 90°$, and apply to connections under branch axial loading.

As shown by the F_2 factor [Eq. (11)], CIDECT DG 8 [5] acknowledges “end effects” on SCFs for CHS-to-CHS axially loaded X-connections with low α (based on research by [24]). For typical axially loaded CHS-to-CHS X-connections, the factor F_2 is plotted against α in Figs. 4a,b. As shown therein, F_2 can be quite small, indicating that “end effects” (according to CIDECT DG 8[5]) can reduce SCFs (significantly) in CHS-to-CHS X-connections. However, $\alpha = 4$ is still large for a practical “end connection” [13] and that Eq. (11) still caters to connections that are symmetrical about the branch(es).

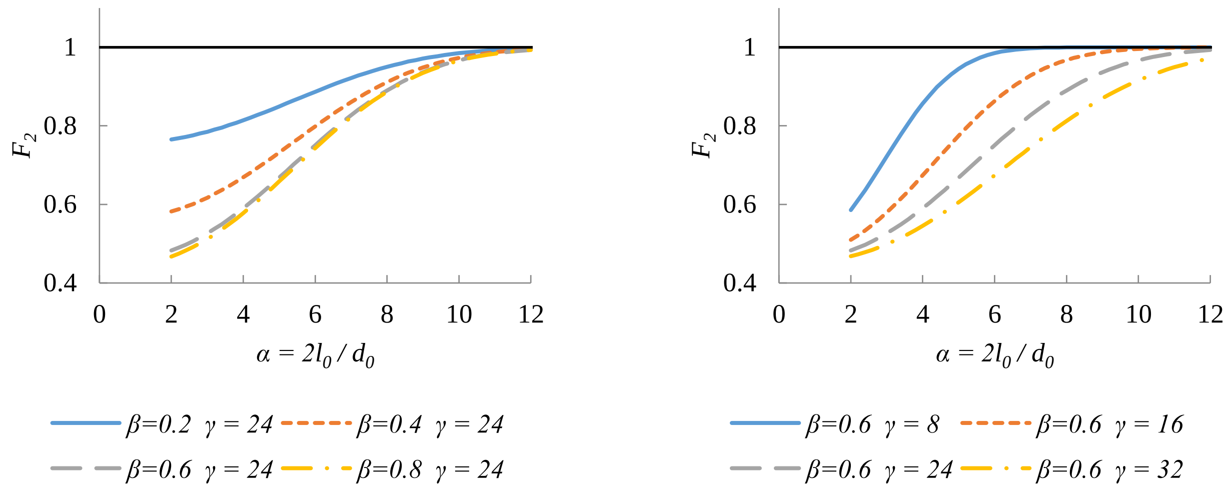

(a) Effect of β (γ = 24) (b) Effect of γ (β = 0.6)

Fig. 4. Effects of chord length and non-dimensional parameters on SCFs in CHS-to-CHS axially loaded X-connections based on CIDECT DG8 [5]

3.2. RHS T- and X-Connections

For "standard" RHS-to-RHS axially loaded T- and X-connections, the CIDECT DG8 [5] formulae for SCFs consider six critical (hot spot) stress locations. These locations are labelled A – E in Fig. 5.

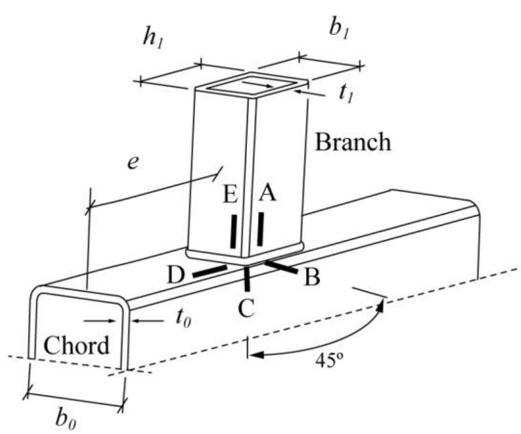

Fig. 5. Critical (hot spot) stress locations for RHS-to-RHS T- and X-connections [5]

The formulae given in CIDECT [5] to calculate SCFs at the "hot spots" (A – E) are:

- For the chord:

$$SCF_B = \left(0.143 - 0.204\beta + 0.064\beta^2\right)\left(2\gamma\right)^{\left(1.377+1.715\beta-1.103\beta^2\right)} \tau^{0.75} \quad (12)$$

$$SCF_C = \left(0.077 - 0.129\beta + 0.061\beta^2 - 0.0006\gamma\right)\left(2\gamma\right)^{\left(1.565+1.874\beta-1.028\beta^2\right)} \tau^{0.75} \quad (13)$$

$$SCF_D = \left(0.208 - 0.387\beta + 0.209\beta^2\right)\left(2\gamma\right)^{\left(0.925+2.389\beta-1.881\beta^2\right)} \tau^{0.75} \quad (14)$$

where SCF_B, SCF_C, and SCF_D = chord SCFs at hot spot B, C, and D, respectively.

- For the branch(es):

$$SCF_A = SCF_E = \left(0.013 + 0.693\beta - 0.278\beta^2\right)\left(2\gamma\right)^{\left(0.790+1.898\beta-2.109\beta^2\right)} \quad (15)$$

where $SCF_A = SCF_E$ = branch SCF at hot spots A and E, respectively.

For connections with fillet welds, SCF_A and SCF_E are multiplied by 1.4, and for X-connections with β = 1.0, SCF_C is multiplied by 0.65 and SCF_D is multiplied by 0.50.

According to CIDECT [5], Eqs. (12)-(15) are valid within the range $0.35 \le \beta \le 1.0$, $12.5 \le 2\gamma \le 25$, $0.25 \le \tau \le 1.0$, for connections under branch axial loading. And, as the factor F_2 is absent, there is no benefit/penalty for "end effects". Part of this issue, concerning end effects for RHS-to-RHS axially loaded X-connections near an open chord end, is herein addressed. It should be noted that, unlike Eqs. 6-8, the CIDECT DG8 formulae for RHS-to-RHS connections are not functions of the branch-to-chord angle.

4. SCFs for RHS X-Connections near an Open Chord End

4.1. Experimental Testing

Two large-scale, directly welded RHS-to-RHS axially loaded X-connections were tested in this research. Their general layout is shown in Fig. 6. The connections were fabricated with RHS members produced to CSA G40.20/G40.21 [25] Grade 350W Class C; they were symmetrical about the branches and had $e = 3b_0$ (on each side) (see Fig. 6). The branch and chord members were joined by partial joint penetration groove welds, using a semi-automatic flux cored arc welding process (the most common process in high-production structural welding). Nominal geometrical properties of the connections are given in Table 1. The specimen IDs (first column in Table 1) are described in the footnote.

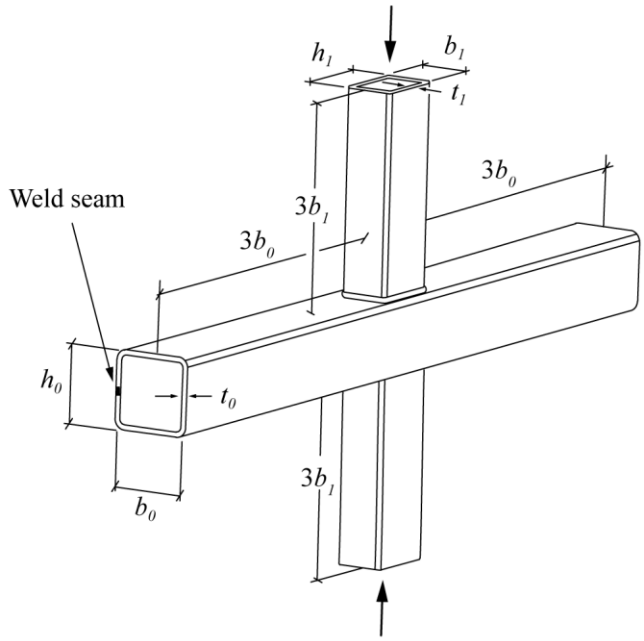

Fig. 6. Layout of test specimens

Table 1. Nominal geometrical properties of test specimens

Specimen ID[1]	Chord ($b_0 \times h_0 \times t_0$) (mm×mm×mm)	Branch ($b_1 \times h_1 \times t_1$) (mm×mm×mm)	$\beta = b_1/b_0$	$2\gamma = b_0/t_0$	$\tau = t_1/t_0$
X-0.5	178×178×12.7	89×89×9.53	0.5	14	0.75
X-0.7	178×178×12.7	127×127×9.53	0.7	14	0.75

[1] ID: connection configuration (i.e. “X”) - β-ratio.

The aim of this initial, experimental work was to produce test results that could be used to validate subsequent FE models. Hence, a procedure recommended by CIDECT DG8 [5], and used in previous test programs (with similar aims) [26,27], was adopted.

Quasi-static axial compression was applied to the end of each branch by using a Universal Testing Machine (UTM) (Fig. 7a), under force control, at a rate of 10 kN/min. For both tests, the load was paused at four stages (30, 40, 50 and 60 kN). At each stage, the connections remained elastic (this was verified by previous FE modelling), and strain concentration factors (SNCFs) were determined. SNCFs are defined as the ratio: hot spot strain / branch nominal strain [5]. Linear strain gauges (SGs) (four total) were installed at the mid-walls of one RHS branch (in each connection) to determine branch nominal strain. These were taken as the average over the four SG readings. Hot spot strains were determined using “chain strain gauges” (CSGs), situated along lines A1

– E1 and A2 – E2 (see Figs. 7b,c), and within the dimensions $L_{r,min}$ and $L_{r,max}$ recommended by CIDECT DG8 [5] (see Fig. 8). These dimensions ($L_{r,min}$ and $L_{r,max}$) are defined by CIDECT DG8 [5] as follows: $L_{r,min}$ is the greater of 0.4 times t_0 or t_1 (for CSGs on the chord and branch, respectively) and 4 mm, and $L_{r,max}$ is equal to $L_{r,min}$ plus t_0 or t_1 (again, for CSGs on the chord and branch, respectively).

Using quadratic extrapolation (in accordance with CIDECT DG8 [5]), the measured strains obtained with the CSGs were used to the calculate hot spot strains and the corresponding SNCFs. Then, the average SNCF (at each of six locations, A – E) was calculated by taking an average of the values on each side of the connection across all load levels. The average SNCFs, for connections X-0.5 and X-0.7, are plotted as filled diamonds in Fig. 9.

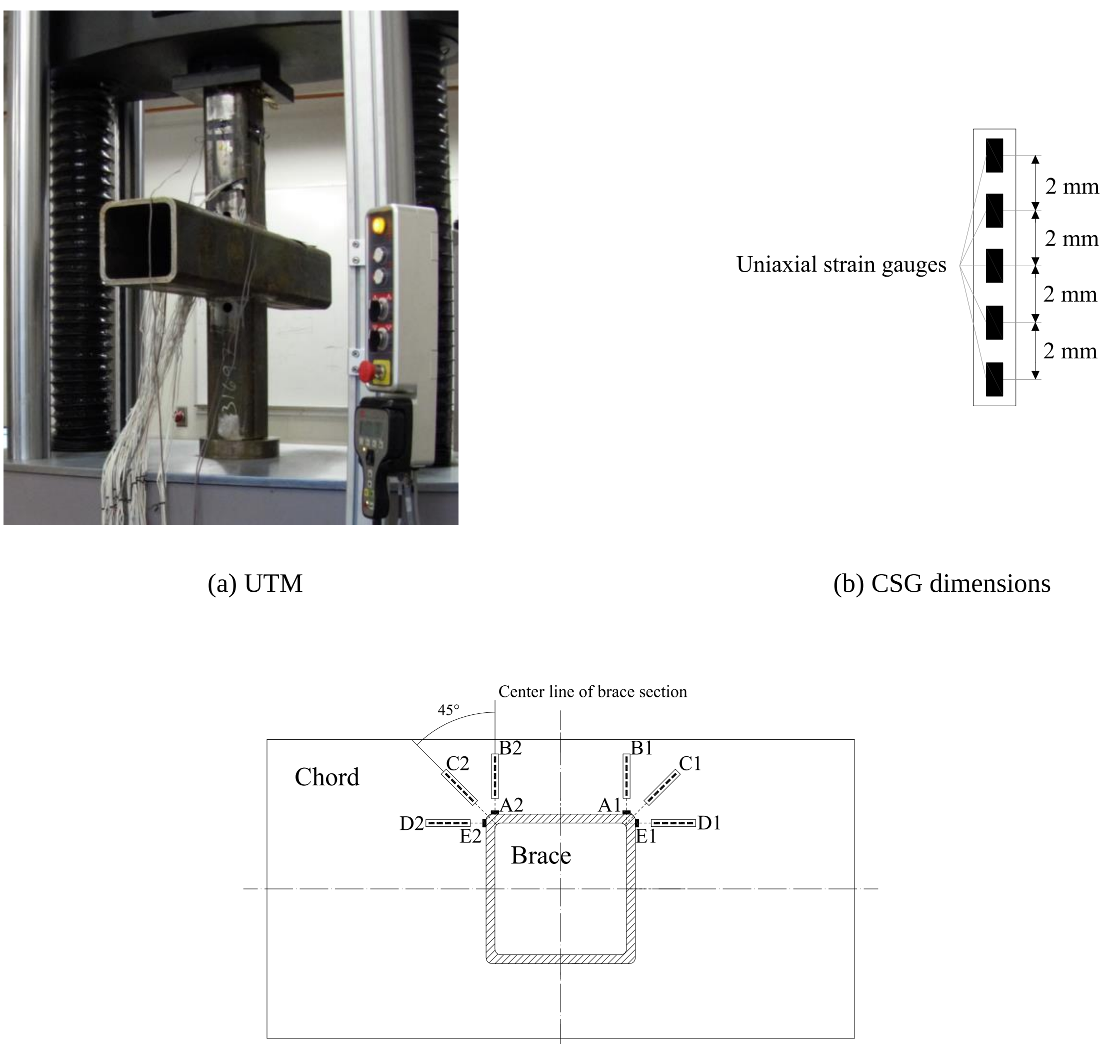

(a) UTM

(b) CSG dimensions

(c) CSG locations

Fig. 7. Test setup and instrumentation

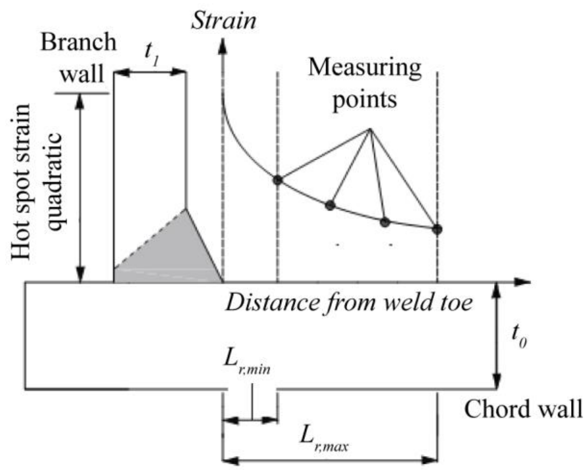

Fig. 8. Strain vs. distance from the weld toe (adapted from [5])

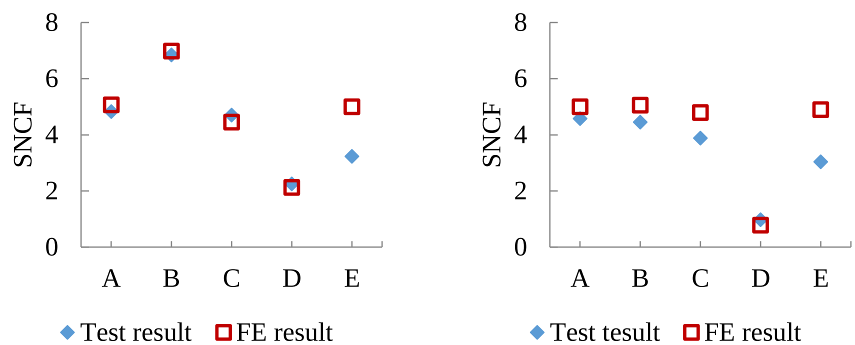

$\frac{\text{Test result}}{\text{FE result}}$ Mean = 0.938 COV = 0.185

(a) X-0.5

$\frac{\text{Test result}}{\text{FE result}}$ Mean = 0.894 COV = 0.252

(b) X-0.7

Fig. 9. Comparison of SNCFs values obtained from experiments and FE analyses

4.2. Finite Element Modelling

Two FE models were developed in ABAQUS [29] to replicate the nominal geometrical properties of the RHS-to-RHS axially loaded X-connections described in Table 1. For both models, the inner and outer corner radii of the RHS members (r_i and r_o, respectively) were taken as one and two times the nominal wall thickness, and the total chord length (l_o) was taken as $6b_0$+b_1 (i.e. e = $3b_o$ on both sides of the connection, as shown in Fig.

6, like the experiments). The modelled weld geometry followed Fig. 10 (which corresponds to the weld geometry in the experiments and in previous studies [27,28,30]).

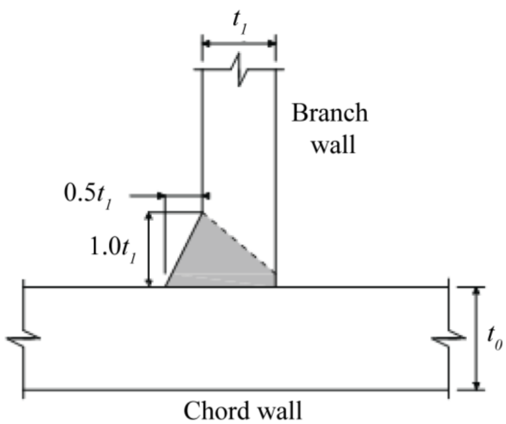

Fig. 10. Weld dimensions (adapted from [27,28,30])

The FE models were partitioned in order to allow calculation of the SNCFs at the locations A1 – E1 and A2 – E2 (see Fig. 7c, shown previously). The region partition of a typical FE model is shown in Fig. 11a. Locations A2 – E2 are not shown in Fig. 11a, but they can be inferred from Fig. 7c. Linear elastic material properties [Young's modulus (*E*) = 200 GPa and Poisson's ratio = 0.3] were applied to the RHS branch(es), chord, and weld materials in accordance with approaches used by previous investigators [26-28,30].

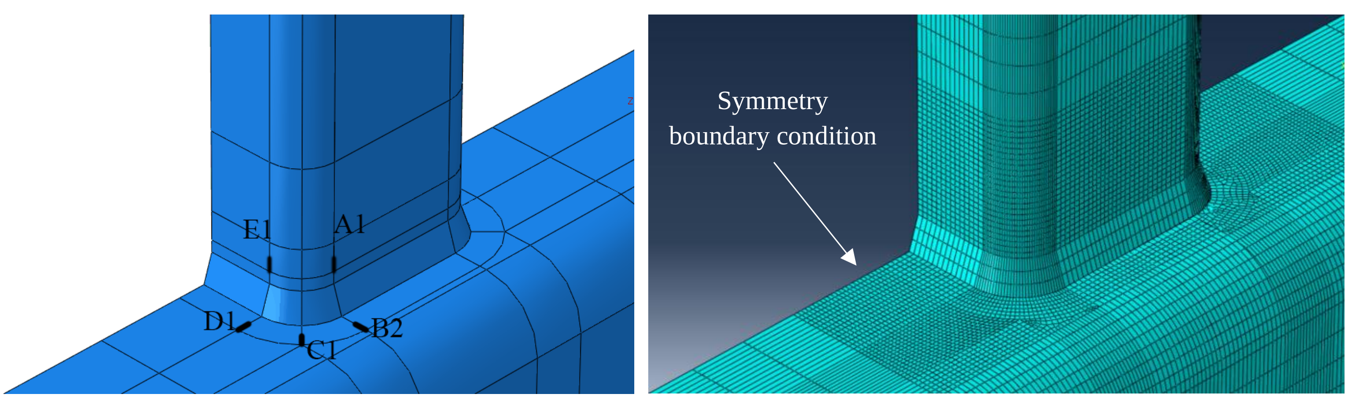

(a) Region partition (b) Mesh pattern at joint location

Fig. 11. FE model details

Four layers of through-thickness solid elements (C3D20R in ABAQUS) were used for the branch(es) and the chord, and a "one-half model" (which was permissible due to symmetry in geometry, loading and boundary conditions along the "cut face"), as shown in Fig. 11b, was used. A "symmetry boundary condition" was applied to all nodes on the "cut face". The nodes at the bottom of the lower branch were "fixed", and the nodes at the top of the upper branch were "free", with loads applied thereto in compression.

For both FE models, SNCFs were obtained by dividing the hot spot strains (calculated using "quadratic extrapolation" [5]) by the branch nominal strain (taken as the applied force divided by the branch cross-sectional area multiplied by E, under a 50 kN axial compression force in the branch). These are compared to SNCFs from the experiments in Figs. 9a,b (where they are plotted as unfilled squares), and show good agreement with them (hence, validating the FE models). A preliminary FE study on "end effects" in RHS-to-RHS axially loaded X-connections near an open chord end was thus performed by using the validated models.

4.2.1. *Preliminary Study on End Effects*

Two "control models", with different β, and $e = 3b_0$, served as the basis for the preliminary study. From each of the two "control models", three new models were created with $e = b_0$, $0.5b_0$ and $0.1b_0$ on *one side only* of the connection (i.e. $e = 3b_0$ was maintained on the other side of the connection, as shown in Fig. 12). The lower bound of $0.1b_0$ chosen represents the smallest practical value of e for an "end connection" [13]. Geometrical properties of these eight models are listed in Table 2. The model IDs (first column in Table 2) are described in the footnote. Fig. 13a shows a typical "control models" and Fig. 13b shows a typical "end connection".

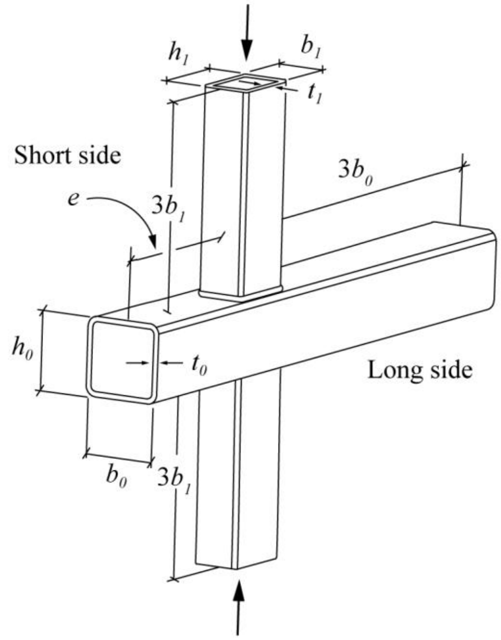

Fig. 12. Schematic diagram of the FE models

Table 2. Geometrical properties of preliminary connection models

Model ID [1]	Chord (b_0×h_0×t_0) (mm×mm×mm)	Branch (b_1×h_1×t_1) (mm×mm×mm)	$\beta = b_1/b_0$	$2\gamma = b_0/t_0$	$\tau = t_1/t_0$	e (mm)
X-0.35-3b_0						600
X-0.35-1b_0	200×200×16	70×70×8	0.35	12.5	0.5	200
X-0.35-0.5b_0						100
X-0.35-0.1b_0						20
X-0.65-3b_0						600
X-0.65-1b_0	200×200×16	130×130×8	0.65	12.5	0.5	200
X-0.65-0.5b_0						100
X-0.65-0.1b_0						20

[1] ID: connection configuration (i.e. "X") - β-ratio – e (see Fig. 12).

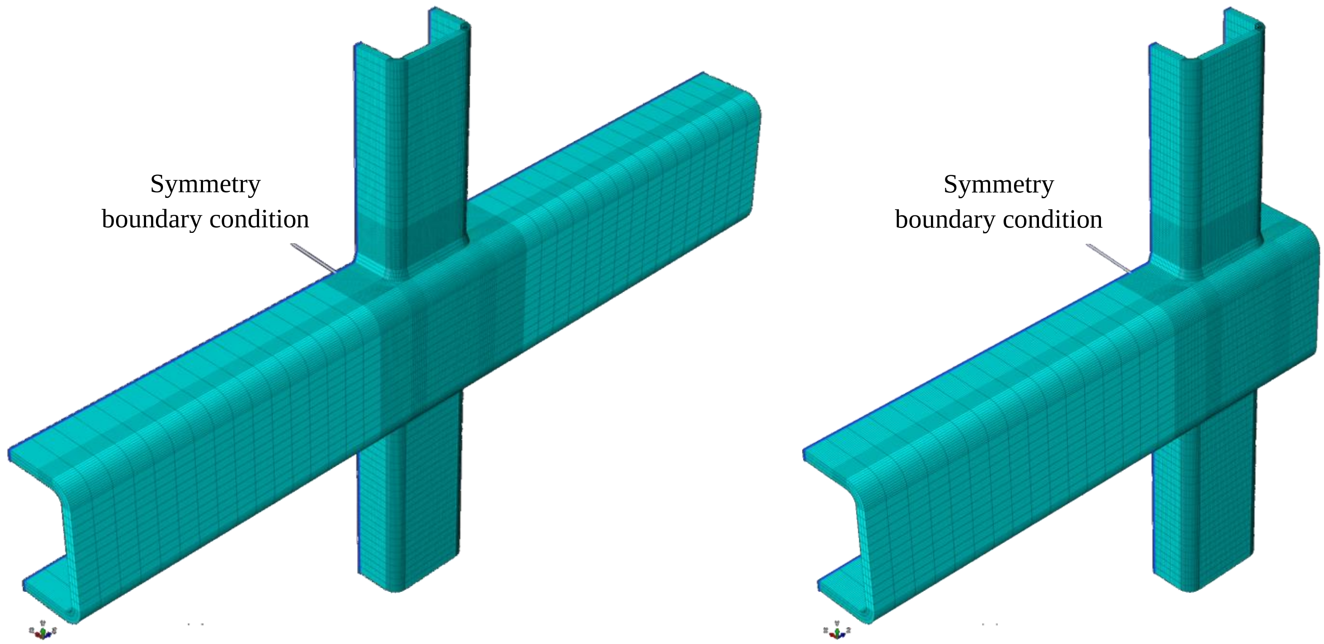

(a) Control model ($e = 3b_0$) (X-0.65-3b_0)

(b) End connection ($e = 0.1b_0$) (X-0.65-0.1b_0)

Fig. 13. RHS-to-RHS axially loaded X-connection models with different end distances

For the "control models", with $e = 3b_0$, the SCF formulae in CIDECT DG8 [5] [i.e. Eqs. (12) to (15)] are theoretically valid. For the "end connections", following the recommendations in Appendix C of CIDECT DG8 for determinations of SCFs by finite element analysis [5], the hot spot stresses at the weld toe at the critical locations A1 – E1 and A2 – E2 (i.e. on both the "long" side and the "short" side of the connection, as labelled in Fig. 11) were calculated using the stress readings within the extrapolation zones. SCFs were then calculated by dividing the hot spot stresses by the nominal stress. The nominal stress was calculated by dividing the branch force by its cross-sectional area.

For the "control models", corresponding SCFs on each side of the connection (e.g. A1 and A2) were the same due to symmetry. For the "end connections", these differed on the "long side" and "short side" of the connection as shown in Fig. 12. The SCFs for all eight connections, at all 12 hot spots, are plotted in Figs. 14 and 15. As pointed out by Efthymiou and Durkin [24], for regular connections, the chord deformation resulting from the branch axial loading decays as the distance from the welded joint increases. If this natural decay is interrupted by using short chords, the SCFs will be affected. It can be seen from Figs. 14 and 15 that "end effects" can reduce SCFs in RHS-to-RHS axially loaded X-connections near an open chord end. This is similar to findings by Efthymiou and Durkin's [24], as implied by the F_2 factor [Eq. (11)] for CHS-to-CHS axially loaded X-connections in CIDECT DG8 [5].

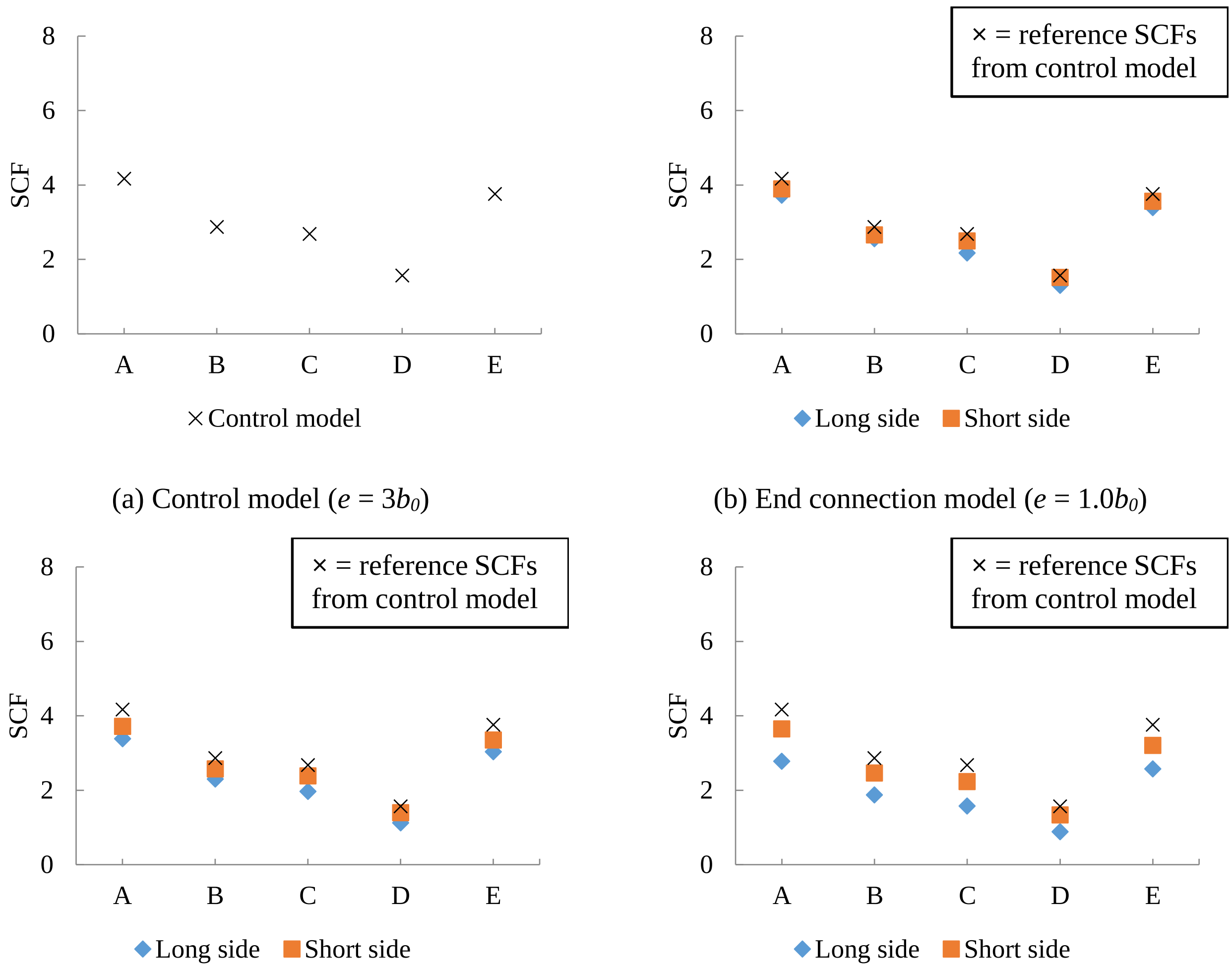

(a) Control model ($e = 3b_0$)

(b) End connection model ($e = 1.0b_0$)

(c) End connection model ($e = 0.5b_0$)

(d) End connection model ($e = 0.1b_0$)

Fig. 14. SCFs for connection models in Table 2 with $\beta = 0.35$

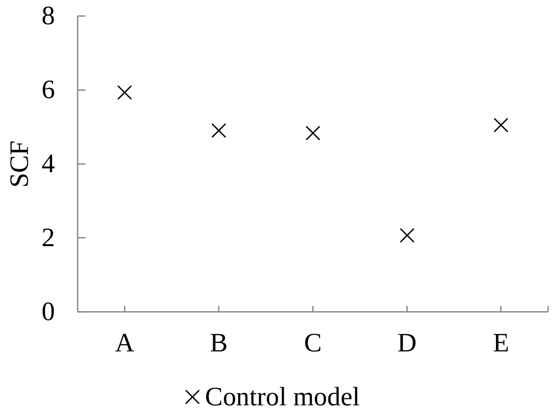

(a) Control model ($e = 3b_0$)

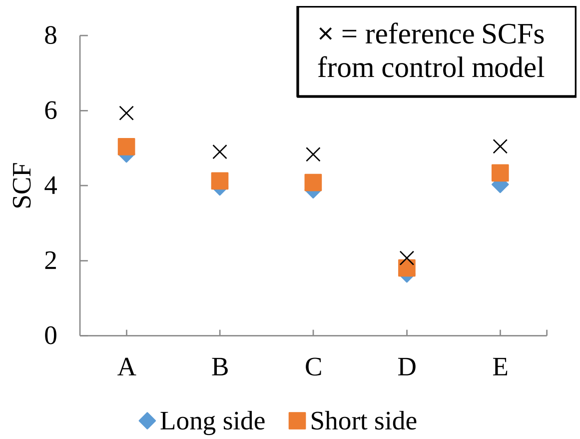

(b) End connection model ($e = 1.0b_0$)

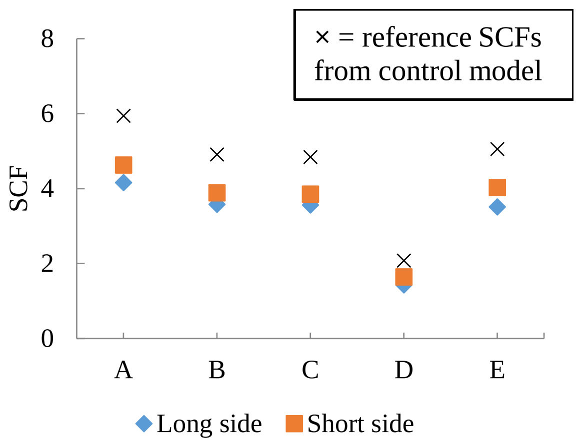

(c) End connection model ($e = 0.5b_0$)

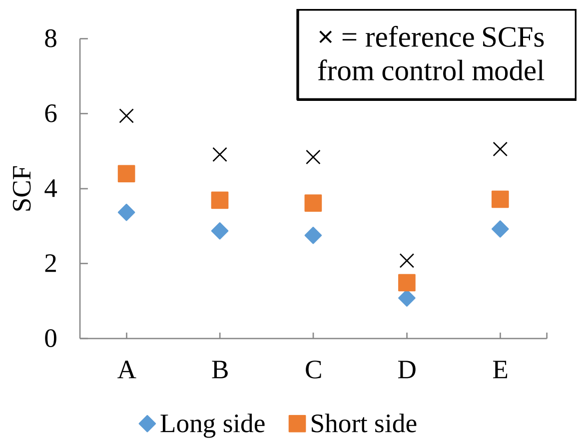

(d) End connection model ($e = 0.1b_0$)

Fig. 15. SCFs for connection models in Table 2 with $\beta = 0.65$

Figs. 14 and 15 also show that the SCFs on the "long side" and the "short side" of the connections are similar, with the SCFs on the "short side" always being slightly greater. This was confirmed for all the FE models in Section 5, where only the SCFs on the "short side" of the connection are presented.

4.3. Parametric Study

Based on the results of the preliminary study, a follow-up (parametric) FE study was deemed necessary to quantify the effect of β, 2γ, τ, and the end distance (e) on SCFs in RHS-to-RHS axially loaded X-connections near an open chord end. The goal of this study was to develop a generalized design approach for RHS-to-RHS axially loaded X-connections (i.e. RHS-to-RHS X-connections under branch axial loading) near an open chord end, for fatigue, using the "hot spot stress method" [5].

The FE parametric study consisted of 256 FE models with chord members of constant outer dimensions ($h_0 = b_0$) of 200 mm. Other dimensions (e.g. t_0, t_1, and l_0) were determined from non-dimensional parameters (β, 2γ and τ), and the end distance (e). Considering the limits of validity of the SCF equations for RHS-to-RHS X-connections in CIDECT DG 8 [5] [Eqs. (12)-(15)], the non-dimensional parameters (β, 2γ and τ) were taken as 2γ = 12.5, 16, 20 and 25; β = 0.35, 0.5, 0.65, and 0.8; and τ = 0.25, 0.5, 0.75, and 1.0. The end distance (e) was varied between $0.1b_0$, $0.5b_0$, $1.0b_0$ and $3.0b_0$, with $3.0b_0$ representing a conservative upper limit for which "end effects" could be safely ignored [13].

4.3.1. ***Results***

For the parametric study, the SCFs in the end connections models are divided by those in the control models. The values are denoted as ψ. Representative results of ψ at the five critical (hot spot) locations on the "short side" of the connections are shown in Figs. 16-18. It can be seen in Fig. 16 that ψ decreases as β increases. Fig. 17 shows that the smaller the 2γ ratio, the smaller are the ψ-values. According to Fig. 18, for different values of e/b_0, the variation in τ has only a minor effect on the the ψ-values. This is consistent with observations by Bu and Packer [13], as well as Eq. (11), which considers "end effects" on SCFs in CHS-to-CHS axially loaded X-connections. [As shown previously, Eq. (11) is a function of 2γ and β, but not τ]. It can also be noted that these plots of ψ vs. e/b_0 in Figs. 16 and 17 exhibit trends similar to those in the plots of F_2 vs. α in Figs. 4a,b.

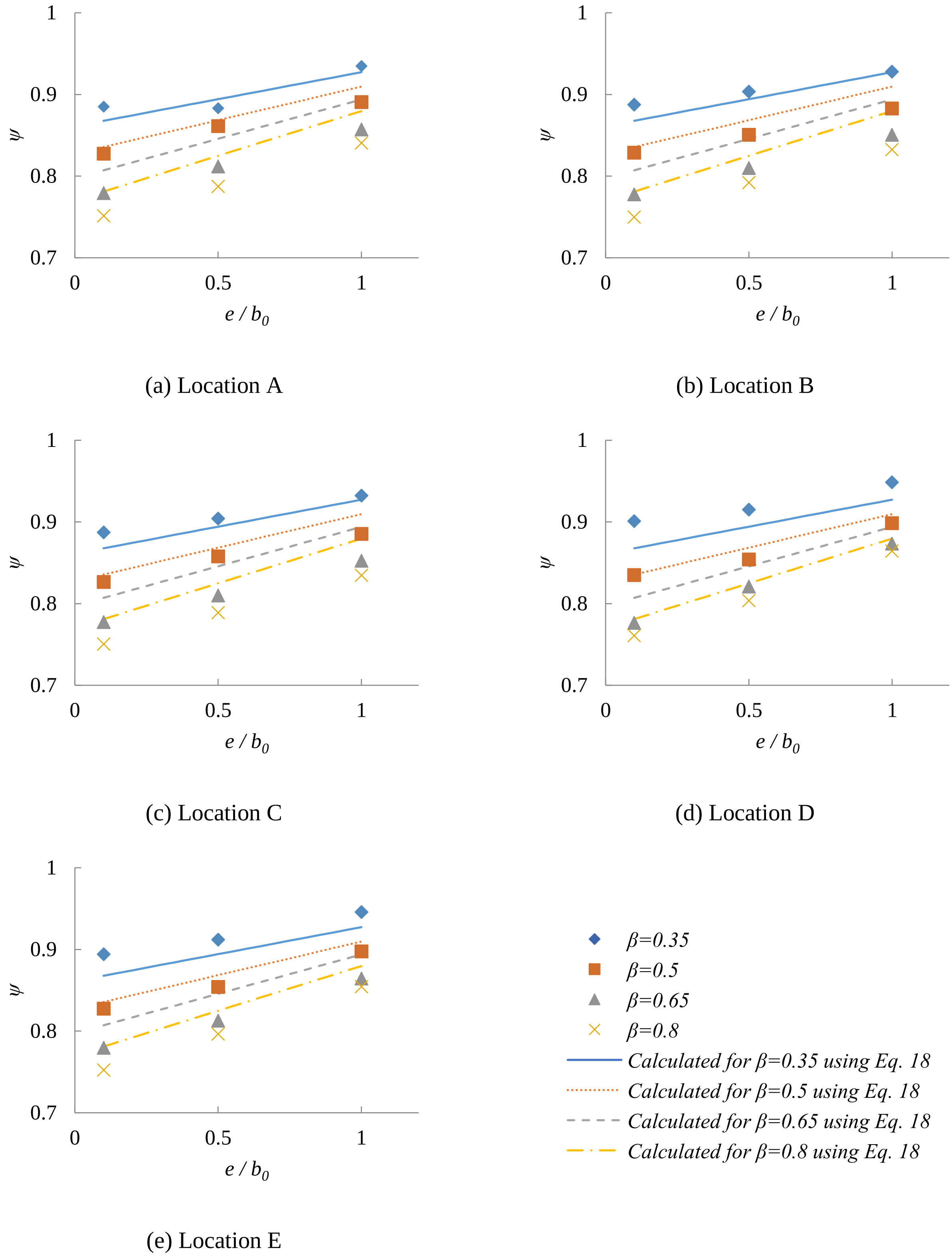

Fig. 16. Effects of e/b_0 and β on SCFs in connections (2γ=20 and τ=0.75)

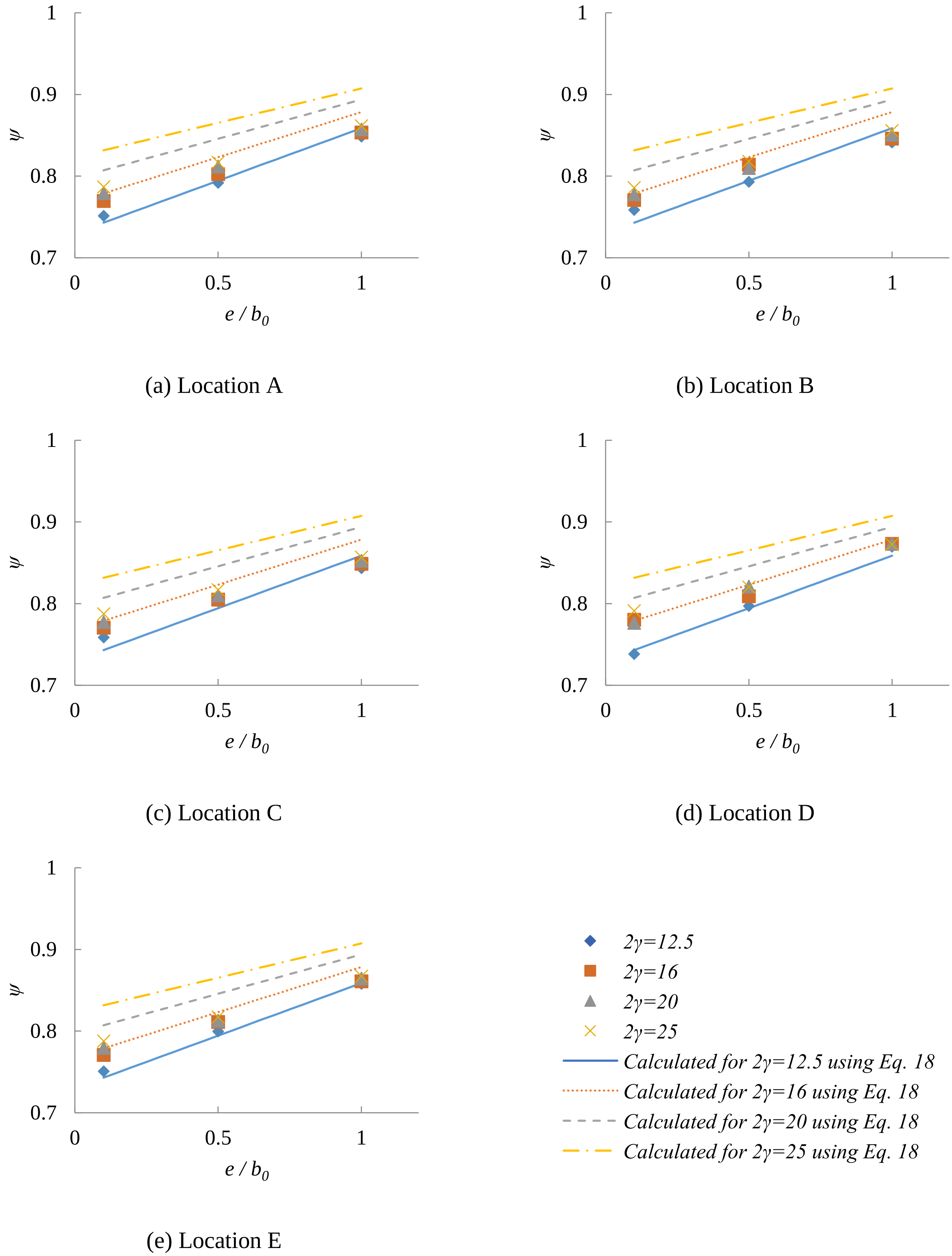

Fig. 17. Effects of e/b_0 and 2γ on SCFs in connections (β=0.65 and τ=0.75)

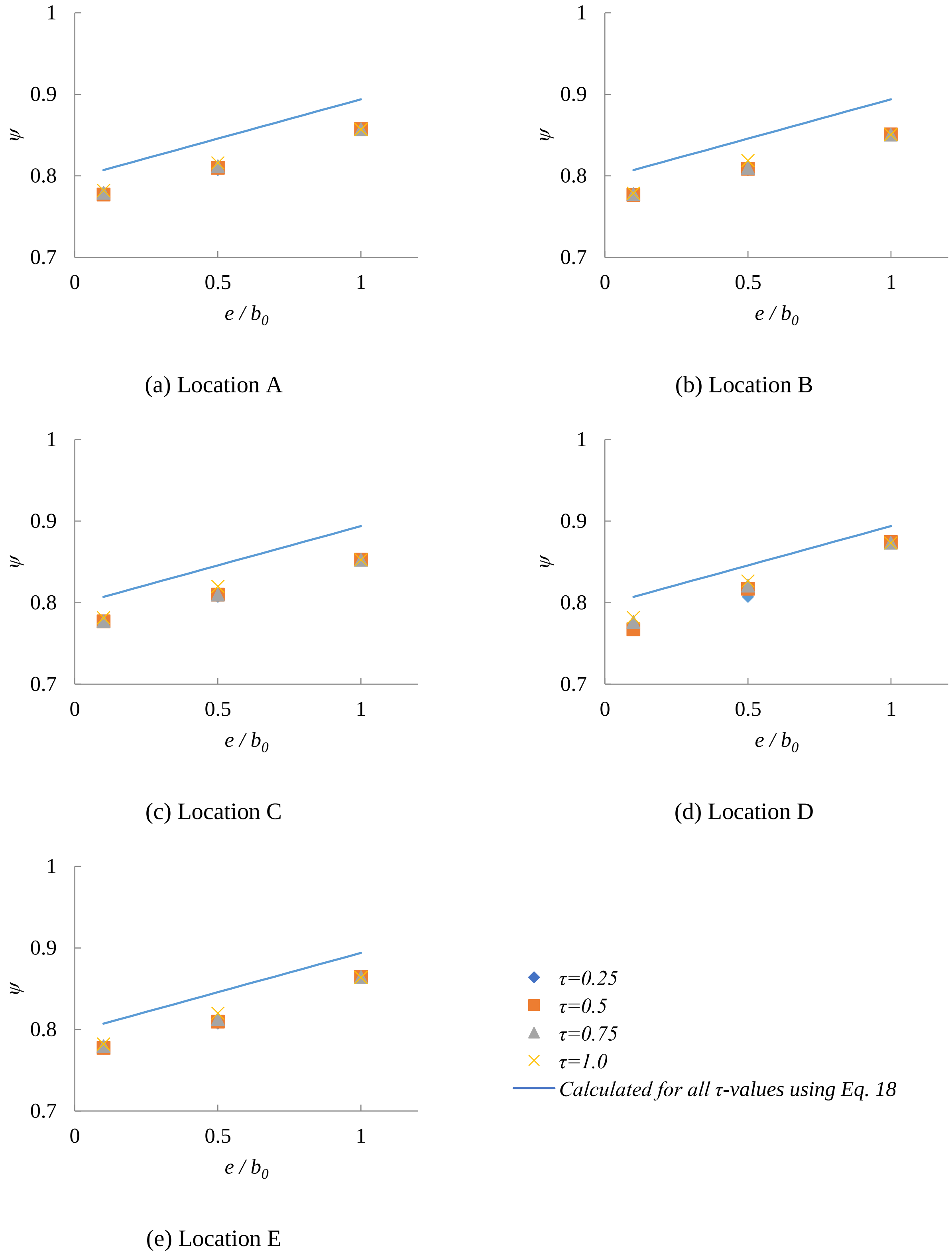

Fig. 18. Effects of e/b_0 and τ on SCFs in connections (β=0.65 and 2γ=20)

5. Design Approach

SCF formulae for directly welded RHS-to-RHS axially loaded X-connections are readily available, such as those recommended by CIDECT DG8 [5]; however, as noted in Section 3.2, they do not consider "end effects". The proposed design approach for RHS-to-RHS axially loaded X-connections (i.e. RHS-to-RHS X-connections under branch axial load) near an open chord end hence aims to utilize existing formulae [Eqs. (12)-(15)] through the introduction of a reduction coefficient (ψ) [like F_2, given by (11)] to consider "end effects"; i.e.:

$$SCF_{end,i} = SCF_i \cdot \psi \tag{16}$$

where $SCF_{end,i}$ = SCF at hot spot i in an RHS-to-RHS axially loaded X-connection near an open chord end; SCF_i = SCF at hot spot i in an RHS-to-RHS axially loaded X-connection [determined using Eq. (12), (13), (14) or (15)]; and i = parameter used to designate a critical (hot spot) location (= A, B, C, D or E).

As discussed in Section 4.3.1, the reduction factors (ψ) for all critical (hot spot) locations (A – E) for the end connection models have been determined by dividing the $SCF_{end,i}$ by SCF_i determined from the corresponding control connections with $e = 3b_0$. For the parametric study, ψ ranges from 0.57 to 0.96.

Also, ψ is nearly constant across all 5 critical (hot spot) locations in each connection, and a mean variation of 1% between ψ at a critical hot spot and the maximum value of ψ at any hot spot in the same connection can be noted. A non-linear regression analysis to relate the maximum value of ψ at any hot spot to non-dimensional connection parameters was hence performed by using Eq. (17) as basis:

$$\psi = 1 - a\left(b - e/b_0\right) / \left(2\gamma/\beta\right)^c \tag{17}$$

where a, b, and c = regression constants.

The arrangement of variables in Eq. (17) was determined empirically and considers the relationships between e/b_o, 2γ and β and the SCFs presented in Figs. 16-18. The values of a, b and c were determined by least-squares regression of 192 data points with e/b_0 = 0.1, 0.5 and 1, 2γ = 12.5, 16, 20 and 25; β = 0.35, 0.5, 0.65, and 0.8; and τ = 0.25, 0.5, 0.75, 1.0. As noted, ψ (the dependent variable) taken as the maximum value of ψ at any hot spot in the same connection (which is hence conservative for all other hot spots). The "best-fit" equation is given by Eq. (18):

$$\psi = 1 - 0.78\left(2.10 - e/b_0\right) \big/ \left(2\gamma/\beta\right)^{0.61} \tag{18}$$

Eq. (18) gives a mean value of actual-to-predicted maximum value of ψ of 1.00 with a COV of 0.03, and a mean value of actual-to-predicted value of ψ (at any hot spot) of 0.99, also with a COV of 0.03. Eq. (18) implies a minimum distance of e = 2.1b_0 to avoid "end effects" on the fatigue life of RHS-to-RHS axially loaded X-connections.

It is hence recommended that Eq. (18) be multiplied by the appropriate SCF equation(s) from CIDECT DG8 [5] (or other design guides) to determine SCFs for RHS-to-RHS axially loaded X-connection near an open chord end. By using previously determined SCF equations for "standard connections", the proposed formula for ψ [Eq. (18)] is expected to provide the same level of reliability for fatigue life predictions of "end connections". The foregoing recommendation is summarized in Fig. 19. To be consistent with CIDECT DG8 [5], a minimum SCF-value of 2.0 is also recommended.

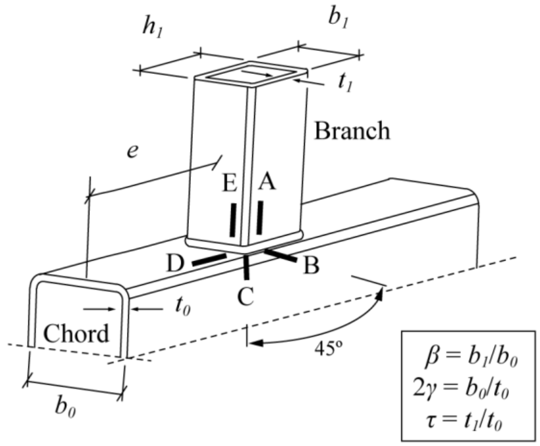

Range of Validity

$0.35 \le \beta \le 1.0$
$12.5 \le 2\gamma \le 25$
$0.25 \le \tau \le 3.0$
and
$0.1 \le e/b_0$

Load Condition: Axial Force on Branch(es)

Chord (lines B, C and D):

$$SCF_B = \left(0.143 - 0.204\beta + 0.064\beta^2\right)\left(2\gamma\right)^{\left(1.377+1.715\beta-1.103\beta^2\right)} \tau^{0.75}\psi$$

$$SCF_C = \left(0.077 - 0.129\beta + 0.061\beta^2 - 0.0006\gamma\right)\left(2\gamma\right)^{\left(1.565+1.874\beta-1.028\beta^2\right)} \tau^{0.75}\psi$$

$$SCF_D = \left(0.208 - 0.387\beta + 0.209\beta^2\right)\left(2\gamma\right)^{\left(0.925+2.389\beta-1.881\beta^2\right)} \tau^{0.75}\psi$$

For X-connections with $\beta = 1.0$:
SCF_C is multiplied by a factor of 0.65, and
SCF_D is multiplied by a factor of 0.50.

Branch (Lines A and E):

$$SCF_A = SCF_E = \left(0.013 + 0.693\beta - 0.278\beta^2\right)\left(2\gamma\right)^{\left(0.790+1.898\beta-2.109\beta^2\right)} \psi$$

For X-connections with fillet welds:
multiply branch SCF_A and SCF_E by 1.40 for the branch side of the weld.

For X-connections with $\beta \le 0.8$:

if $e/b_0 \ge 2.1$: $\psi = 1$

if $e/b_0 < 2.1$: $\psi = 1 - 0.78\left(2.10 - e/b_0\right) / \left(2\gamma/\beta\right)^{0.61}$

Otherwise:

$$\psi = 1$$

Fig. 19. Recommended SCFs for RHS-to-RHS axially loaded X-connections

6. Conclusions

An FE parametric study consisting of 256 linear FE models was conducted to determine SCFs for directly welded RHS-to-RHS axially loaded X-connections near an open chord end. The FE analyses were validated by comparison to two large-scale (experimental) tests. The following conclusions are made:

(1) SCFs in RHS-to-RHS axially loaded X-connections near an open chord end are lower than those in "standard" RHS-to-RHS X-connections with sufficient chord continuity (i.e. $e/b_0 \geq 2.1$ on both sides of the connection, as determined in this study);

(2) SCFs in RHS-to-RHS axially loaded X-connections near an open chord end become smaller (and hence less critical) as e/b_0 becomes smaller, and as 2γ becomes larger;

(3) The highest SCFs in RHS-to-RHS axially loaded X-connections near an open chord end are found in connections with medium values of β; and

(4) For different value of $e/b_0 \leq 2.1$, τ has a negligible effect on the SCFs.

SCF reduction factors (ψ) were derived from the FE results and regression analyses were conducted to derive a parametric formula to estimate ψ based on e/b_0, 2γ and β. As demonstrated in Fig. 20, the ψ formula derived from this work can be used in conjunction with existing SCF formulae in CIDECT DG8 [5] (or other design guides) to estimate SCFs for RHS-to-RHS axially loaded X-connections near an open chord end. The results of this study are valid for $0.1 \leq e/b_0 \leq 3.0$, $12.5 \leq 2\gamma \leq 25$, $0.35 \leq \beta \leq 0.8$, and $0.25 \leq \tau \leq 3.0$.

Acknowledgements

The authors would like to express their appreciation to the Natural Sciences and Engineering Research Council of Canada (NSERC) for providing the financial support for this research.

Nomenclature

E	Young's modulus
$L_{r,max}$	distance from weld toe to end point of extrapolation zone
$L_{r,min}$	distance from weld toe to starting point of extrapolation zone
SCF_A	branch SCF at hot spot A
SCF_B	chord SCF at hot spot B
SCF_C	chord SCF at hot spot C
SCF_D	chord SCF at hot spot D
SCF_E	branch SCF at hot spot E
$SCF_{b\_crown,ax}$	branch SCF at the crown point
$SCF_{b\_saddle,ax}$	branch SCF at the saddle point
$SCF_{ch\_crown,ax}$	chord SCF at the crown point
$SCF_{ch\_saddle,ax}$	chord SCF at the saddle point
$SCF_{end,i}$	SCF at hot spot *i* in an RHS-to-RHS axially loaded X-connection near an open chord end
SCF_i	SCF at hot spot *i* in an RHS-to-RHS axially loaded X-connection
E	Young's modulus
F_2	reduction factor to account for "end effects" in CIDECT DG8
X_{1-4}	SCF parameter for CHS-to-CHS X-connections
a, b, and c	Regression constants
b_0	chord width
b_1	branch width
d_0	chord diameter
d_1	branch diameter
e	end distance = distance from the heel/toe of the closest branch to the chord end
e_{min}	minimum required end distance
h_0	chord height
h_1	branch height

i parameter used to designate a critical (hot spot) location (i = A, B, C, D or E)

l_0 chord length

r_i inner corner radius

r_o outer corner radius

t_0 chord wall thickness

t_1 branch wall thickness

α chord length parameter (= $2l_0/b_0$ or $2l_0/d_0$)

β branch-to-chord width ratio (= b_1/b_0); branch-to-chord diameter ratio (= d_1/b_0)

γ half chord width-to-thickness ratio (= $b_0/2t_0$); half chord diameter-to-thickness ratio (= $d_0/2t_0$)

τ branch-to-chord thickness ratio (= t_1/t_0)

θ acute angle between the branch and chord (in degrees)

ψ reduction factor for end connection

References

[1] J.A. Packer, J.E. Henderson, Hollow Structural Section Connections and Trusses – a Design Guide, 2nd ed. Canadian Institute of Steel Construction, Toronto, Canada, 1997.

[2] J. Wardenier, Y. Kurobane, J.A. Packer, A. van der Vegte, X.L. Zhao, Design Guide for Circular Hollow Section (CHS) Joints under Predominantly Static Loading, CIDECT Design Guide No. 1, 2nd ed. CIDECT, Geneva, Switzerland, 2008.

[3] J.A. Packer, J. Wardenier, X.L. Zhao, G.J. van der Vegte, Y. Kurobane, Design Guide for Rectangular Hollow Section (RHS) Joints under Predominantly Static Loading, CIDECT Design Guide No. 3, 2nd ed. CIDECT, Geneva, Switzerland, 2009.

[4] ISO (International Organization for Standardization), ISO 14346:2013, Static Design Procedure for Welded Hollow Section Joints – Recommendations, Geneva, Switzerland, 2013.

[5] X.L. Zhao, S. Herion, J.A. Packer, R.S. Puthli, G. Sedlacek, J. Wardenier, K. Weynand, A.M. van Wingerde, N.F. Yeomans, Design Guide for Circular and Rectangular Hollow Section Welded Joints under Fatigue Loading, CIDECT Design Guide No. 8, CIDECT and Verlag TÜV Rheinland GmbH, Köln, Germany, 2001.

[6] ISO (International Organization for Standardization), ISO 14347:2008, Fatigue – Design Procedure for Welded Hollow-Section Joints – Recommendations, Geneva, Switzerland, 2008.

[7] CSA (Canadian Standard Association), CSA S16-19, Design of Steel Structures, Toronto, Canada, 2019.

[8] CSA (Canadian Standard Association), CSA W59-18, Welded Steel Construction, Toronto, Canada, 2018.

[9] AISC (American Institute of Steel Construction), ANSI/AISC 360-16, Specification for Structural Steel Buildings. Chicago, IL, USA, 2016.

[10] J.A. Packer, D.R. Sherman, M. Lecce, Design Guide No. 24, Hollow Structural Section Connections. American Institute of Steel Construction, Chicago, IL, USA, 2010.

[11] AWS (American Welding Society), AWS D1.1/D1.1M:2020, Structural Welding Code – Steel, Miami, FL, USA, 2020.

[12] CEN (European Committee for Standardization), EN 1993-1-8:2010, Eurocode 3: Design of Steel Structures – Part 1–8: Design of Joints, Brussels, Belgium, 2010.

[13] X.D. Bu, J.A. Packer. Chord end distance effect on RHS connections. Journal of Constructional Steel Research, 168 (2020) 105992.

[14] Y.J. Fan, J.A. Packer, RHS-to-RHS axially loaded X-connections near an open chord end. Canadian Journal of Civil Engineering 44 (2017) 881-892.

[15] G.J. van der Vegte, Y. Makino, Further research on chord length and boundary conditions of CHS T- and X-joints. Advanced Steel Construction 6(3) (2010) 879-890.

[16] A.P. Voth, J.A. Packer, Branch plate-to-circular hollow section connections. II: X-type parametric numerical study and design. Journal of Structural Engineering, American Society of Civil Engineers, 138(8) (2012) 1007–1018.

[17] A.P. Voth, J.A. Packer, Numerical study and design of T-type branch plate-to-circular hollow section connections. Engineering Structures 41 (2012) 477–489.

[18] CEN (European Committee for Standardization), Eurocode 3: Design of steel structures – Part 1–8: Design of joints. prEN 1993-1-8:2018, Brussels, Belgium, 2018.

[19] K. Tousignant, Effect of chord length and boundary conditions on welds in CHS X-joints. Proceedings of the 17th International Symposium on Tubular Structures, Singapore (2019) 63-70.

[20] L.M. Connelly & N. Zettlemoyer. Frame behaviour effects on tubular joint capacity. Proceedings of the 3rd International Symposium on Tubular Structures, Lappeenranta, Finland. 1989. pp. 91-89.

[21] H.M. Bolt, H. Seyed-Kebari & J.K. Ward. The influence of chord length and boundary conditions on K-joint capacity. Proceedings of the 2nd International offshore and polar engineering conference, San Fransico, USA, 1992, Vol. IV, pp. 347-354.

[22] Y.S. Choo, X.D. Qian, J. Wardenier, Effects of boundary conditions and chord stresses on static strength of thick-walled CHS K-joints. Journal of Constructional Steel Research 62 (2006) 316-328.

[23] G.J. van der Vegte, Y. Makino, Ultimate strength formulation for axially loaded CHS uniplanar T-joints, International Journal of Offshore and Polar Engineering (2006) 16(4) 305-312.

[24] M. Efthymiou, S. Durkin, Stress concentration in T/Y and gap/overlap K-joints, Proceedings of the 4th International Conference on Behaviour of Offshore Structures, Amsterdam, The Netherlands (1985) 429–440.

[25] CSA (Canadian Standards Association), CAN/CSA-G40.20-13/G40.21-13, General requirements for rolled or welded structural quality steel/structural quality steel. Toronto, Canada, 2013.

[26] R. Feng, B. Young, Stress concentration factors of cold-formed stainless steel tubular X-joints. Journal of Constructional Steel Research 91 (2013) 26-41.

[27] L.W. Tong, G.W. Xu, D.L. Yang, F.R. Mashiri, X.L. Zhao, Stress concentration factors in CHS-CFSHS T-joints: experiments, FE analysis and formulae. Engineering Structures 151 (2017) 406-421.

[28] L.W. Tong, G.W. Xu, Y.Q. Liu, D.Q. Yan, X.L. Zhao, Finite element analysis and formulae for stress concentration factors of diamond bird-beak SHS T-joints. Thin-Walled Structures 86 (2015) 108-120.

[29] Dassault Systèmes, ABAQUS Version 6.14 [Computer software]. Dassault Systèmes, Providence, RI, USA, 2014.

[30] B. Cheng, Q. Qian, X.L. Zhao, Numerical investigation on stress concentration factors of square bird-beak SHS T-joints subject to axial forces. Thin-Walled Structures 94 (2015) 435-445.